Journal of Molecular Structure 1238 (2021) 130406

Contents lists available at ScienceDirect

Journal of Molecular Structure

journal homepage: www.elsevier.com/locate/molstr

Synthesis, structure and basic properties of 5,10,15,20-tetrakis[4′-(*benzoxazole*-2-*yl*)*phenyl*]-21,23-dithiaporphyrin

S.G. Pukhovskaya [a,*], Y.B. Ivanova [b], A.N. Kiselev [b], N.A. Fomina [b], S.A. Syrbu [b]

[a] Ivanovo State University of Chemistry and Technology, 153460, Sheremetevsky Pr. 7, 153000 Ivanovo, Russia
[b] G.A. Krestov Institute of Solution Chemistry of the Russian Academy of Sciences, Akademicheskaya St. 1, 153045 Ivanovo, Russia

ARTICLE INFO

Article history:
Received 14 December 2020
Revised 11 March 2021
Accepted 29 March 2021
Available online 9 April 2021

Keywords:
Synthesis
Heterosubstituted Porphyrins
Basic Properties

ABSTRACT

The synthesis of 5,10,15,20-tetrakis [4 '- (benzoxazol-2-yl) phenyl] -21,23-dithiaporphyrin was carried out by the reaction of metal complex catalysis. In this work, quantum chemical calculations were performed in the DFT approximation (hybrid functional B3LYP) with a set of 6–21 G basis functions. The resulting compound was identified by electron absorption, ^{1}H NMR spectroscopy and mass spectrometry. The basic properties of heterosubstituted ligand in comparison with the classical porphyrin analogue and unsubstituted TPP were studied by the spectrophotometric titration method in an acetonitrile - perchloric acid system. The basicity constants for the first and second steps and the ranges of existence of the protonated forms of 5,10,15,20-tetrakis [4 '- (benzoxazol-2-yl) phenyl] -21,23-dithiaporphyrin and its classical analog were determined.

1. Introduction

Porphyrins are one of the best-studied classes among all known macrocyclic systems [1], but the interest in their studies is far from weakening; instead, it continues to grow. The fact that porphyrins and their analogues have such diverse properties is associated with their specific molecular structure [1-5]. Finding solutions to the fundamental problems related to this class of compounds and their practical applications are directly dependent on the optimization of the porphyrin synthesis methods and possibility of chemical modification [6]. There are two methods of porphyrin macrocycle transformation. One is the substitution of the hydrogen atoms in the β-positions of the pyrrole rings, in the *meso*positions and at the transannular nitrogen atoms of the macrocycle. The variety of organic and inorganic groups that can be chosen as substituents makes it possible to obtain a large number of classical porphyrin structures [7-10]. The second method of macrocycle transformation is changing the macrocycle itself through hydrogenation, broadening the conjugation system by adding carbo- or heterocycles and through replacing one or two transannular nitrogen atoms with other donor atoms: O, C, S, Se, and Te [11]. The result of such transannular modification is porphyrinoids or heterosubstituted porphyrins, with properties considerably different from those of classical porphyrins.

It is well known that the synthesis of porphyrins with heterocyclic substituents is based on the condensation of heterocyclic aldehydes that are often difficult to obtain or that produce a low yield of the final macroheterocycle. A breakthrough in the preparation of such macroheterocycles was made with the discovery of cross-coupling reactions [12]. The development of the cross-coupling method enabled C–H-functionalization of macrocycles catalyzed by transition metal complexes [13].

Porphyrins and related macroheterocyclic compounds are applied in a variety of technological fields as catalysts of practically important processes, as parts of materials for optical limiters, photosensitizers, solar energy converters, and many other devices [3,6,14,15]. The last few years have seen a rapid development of the porphyrin application areas, such as diagnostics and treatment of malignancies, anemia, neuropsychic disorders; skin, eye, and many other diseases [16-19].

Introduction of various heterocyclic substituents and donor atoms into the porphyrin macrocycle has a great effect on the porphyrin electronic structure and, thus, changes the physical and chemical properties of the compounds, preserving their aromaticity. When biologically active molecules are used as substituents, they improve the useful properties of a compound as a whole. A serious problem in medicine is the fast emergence of drug-resistant microbial strains. Since the emergence of antiresistant bacteria is inevitable, it is absolutely urgent to discover new active agents; and among them, benzoxazole derivatives are the most promising candidates [20,21]. This work presents the results of the synthesis of 5,10,15,20-tetrakis[4′-(*benzoxazole*-2-*yl*)*phenyl*]−21,23-

* Corresponding author.
E-mail address: svetlana.puhovskaya@mail.ru (S.G. Pukhovskaya).

https://doi.org/10.1016/j.molstruc.2021.130406
0022-2860/

dithiaporphyrin (**I, S_2TPP**) and the study of its spectral, acid-base properties in comparison with the earlier synthesized classical analogue - 5,10,15,20-tetrakis[4′-(*benzoxazole*-2-*yl*)*phenyl*]porphyrin (**II, H_2PP**) [13] - and the easiest to obtain synthetic porphyrin - 5,10,15,20-tetraphenylporphin (**III, H_2TPP**).

2. Experimental

2.1. Materials and equipment

The solvents used in this work (perchloric acid, acetonitrile, dichloromethane, toluene, tetrahydrofuran, *para*-xylene, and methanol) were purified by the standard methods [22]. Benzaldehyde, 4-bromobenzaldehyde, trifluoroacetic acid, benzoxazole, palladium acetate, palladium tetrakis(triphenylphosphine), copper acetate, potassium carbonate, potassium hydroxide, triphenylphosphine, and pyrrole produced by Aldrich were used without purification.

For preparative column chromatography, a Merck silica gel with a particle size of 40–60 μm was used. The compound individuality was controlled by the TLC method employing Silufol plates with a layer thickness of 0.5 mm (Merck) and dichloromethane as the eluent (the dichloromethane /methanol ratios were 50:1, 100:1). The UV–visible spectra were measured on *Shimadzu UV-1800* and *Hitachi U-2000* spectrophotometers. The acid-base properties of the porphyrins were studied by spectrophotometric titration. The experimental techniques and methods of experimental data processing are presented in detail in work [23].

Chemically pure perchloric acid (58% aqueous solution), which has a high dissociation constant (pKa. = 2.8 [24]) in acetonitrile, was used as the protonating agent. For titration, a working 0.01 M solution of perchloric acid ($HClO_4$) in acetonitrile was prepared. The error in the measurement of the corresponding constants was ± 3–5%.

2.2. Synthesis

2.2.1. Synthesis of 5,10,15,20-tetrakis(4′-bromophenyl)porphin

2.0 mL of trifluoroacetic acid and 150.0 mL of *para*-xylene were placed into a 1 L three-neck flask equipped with a Dean-Stark trap, a reflux condenser, an air feed pipe, and a dropping funnel. The mixture was heated to the *para*-xylene boiling point and a solution of 13.3 g (72 mmol) of 4-bromobenzaldehyde and 5 g (72 mmol) of pyrrole was added from the dropping funnel to 150 mL of *para*-xylene, with air simultaneously passed through the mixture.

The reaction mixture was boiled for 1 hour, with air simultaneously passed through it. Then the mixture was cooled to room temperature, 2 mL of diethanolamine were added, and after that, the mixture was left overnight. Then the porphyrin precipitate was filtered, washed with ethanol, and dried at room temperature until its weight became constant. For purification, the porphyrin was dissolved in dichloromethane and chromatographed on aluminum oxide, Brockman activity grade II, with simultaneous dichloromethane elution. The porphyrin eluate was evaporated and precipitated with ethanol. Yield: 5.9 g (35%).

^{1}H NMR ($CDCl_3$, 500 MHz): δ −2.85 (bs, 2H, NH), 7.92 (d, 8H, J = 8.0 Hz, Ar), 8.10 (d, 8H, J = 8.0 Hz, Ar), 8.87 (s, 8H, H-pyrrole).

Elemental analysis: calculated:% H 2.820; C 56.810; N 6.02; Br 34.35; determined experimentally:%H 2468; C 56,595; N 5632; Br 34,35.

UV–vis: λ_{max}, nm (lgε): 650(3.95), 590(3.89), 549(4.04), 515(4.34), 419(5.68) ($CHCl_3$).

MALDI-TOF MS: *m/z* calculated: $C_{44}H_{26}Br_4N_4$, 929.8911; determined experimentally: 929.6612 [M]+.

2.2.2. Synthesis of 5,10,15,20-tetrakis[4′-bromophenyl]−21,23-dithiaporphyrin

Five grams (11 mmol) of 2,5-bis-(4′-bromophenyl hydroxymethyl)thiophene, 150 mL of *para*-xylene, and 0.75 mL (11 mmol) of pyrrole were placed into a 250 mL three-necked round-bottomed flask equipped with a Dean-Stark trap, a reflux condenser, and an air feed pipe. Then the mixture was heated to the *para*-xylene boiling point and 1 mL of trifluoroacetic acid was added from the dropping funnel to 50 mL of *para*-xylene, with air simultaneously passed through the mixture. The mixture was boiled for 1 h and the *p*-xylene was distilled off with water vapor. Then the precipitate was filtered, washed with water and dried at room temperature until its weight became constant. The raw product was dissolved in dichloromethane and chromatographed on silica gel with simultaneous dichloromethane elution. The second brownish-orange dithiaporphyrin layer was collected, the eluate was evaporated, the product was precipitated with methanol, filtered and dried at room temperature until its weight became constant. Yield: 0.63 g (12%). For further purification, the product was chromatographed on silica gel again.

^{1}H NMR ($CDCl_3$, 500 MHz) δ, ppm: 9.73 (s,4H, β-H), 8.69 (s, 4H, β-H), 8.16 (d, 8H, J = 7.94 Hz, Ar), 8.03d (d, 8H, J = 7.32 Hz, Ar).

MALDI-TOF MS: *m/z* calculated: $C_{44}H_{24}Br_4N_2S_2$: 966.1100; determined experimentally: 966.1080 [M]+.

2.2.3. Synthesis of 5,10,15,20-tetrakis[4′-(benzoxazole-2-yl)phenyl]−21,23-dithiaporphyrin(I)

First, 4.15 mg $Pd(OAc)_2$ (40 mol%), 3.69 mg $Cu(OAc)_2$•H_2O (40 mol%), 30.3 mg triphenylphosphine (2.5 eq.), 44.68 mg 5,10,15,20-tetrakis[4′-*bromophenyl*]−21,23-dithiaporphin (0.0463 mmol), (3 mL) toluene, and 44.72 mg benzoxazole (8 eq. 0.3704 mmol) were placed into a 5 mL flask equipped with a magnetic stirrer and a reflux condenser. Then the mixture was stirred for 1 min; 31.99 mg of potassium carbonate (5 eq.) were added. After that, the mixture was stirred again and was simultaneously boiled. Forty hours later, when the reaction was completed, the reaction mixture was cooled to room temperature and dichloromethane (5 mL) was added. The mixture was filtered off, the precipitate was washed portionwise with dichloromethane (2 × 5 mL), and the combined organic fractions were evaporated in a vacuum. To obtain chemically pure compounds, the residue was chromatographed on silica gel, which was accompanied by its elution with a dichloromethane-methanol mixture (100:1). Yield: 23.7 mg (46%).

^{1}H NMR (CDCl3, 500 MHz): 9.86 (s, 4H, β-H-thiophene), 8.83 (s, 4H, β-H-pyrrole), 8.59 (s, 4H, β-H), 8.22–8.25 (m, 8H 3 J = 7.8 Ar), 7.75–7.49 (m, 8H, 3 J = 7.8 Hz Ar).

MALDI-TOF MS: *m/z* calculated: $C_{72}H_{40}N_6O_6S_2$: 1118.2611; Determined experimentally: 1118.2411 $[MH]^+$.

2.2.4. Synthesis of zinc 5,10,15,20-tetrakis[4-(1,3-benzoxazole-2-yl)phenyl]porphyrinate (II)

Porphyrin (**II**) was synthesized using the method described in work [13]. The compound chemical purity was controlled by the TLC method using Silufol plates with the layer thickness of 0.5 mm ("Merck'), and employing dichloromethane as the eluent. The spectral characteristics of the compound agreed with the literature data [13].

Yield: 8 mg (14%), vinous-green crystalline powder. UV-visible, λ_{max}, nm (log ε): 427(5.90); 553(4.81); 596(4.67) (dichloromethane). ^{1}H NMR δ, ppm: 7.40–7.46 m (8H); 7,67–7,71 m (4H); 7,84–7.88 m (4H); 8.40d (8H, 3 J = 7.7 Hz); 8.64d (8H, 3 J = 7.7 Hz); 9.02 s (8H) ($CDCl_3$).

MALDI-TOF MS: *m/z* calculated: $C_{72}H_{40}N_8O_4Zn$: 1144.25; determined experimentally: 1144.22 $[M]^+$.

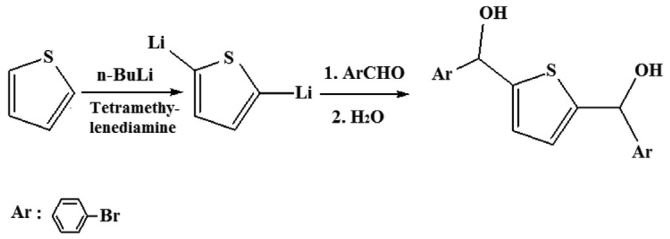

Scheme 1. The first stage.

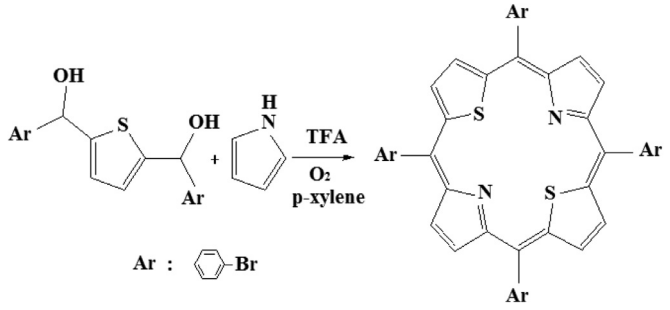

Scheme 2. The second stage.

To obtain metal-free ligand (**II**), the solution of the zinc complex was treated with an HCl solution in dichloromethane, washed with water until a neutral reaction, and chromatographed on silica gel, which was accompanied by its elution with CH_2Cl_2.

MALDI-TOF MS: *m/z* calculated: $C_{72}H_{42}N_8O_4$: 1080.86; determined experimentally: 1080.82 $[M]^+$.

Zinc **5,10,15-tris[4-(1,3-*benzoxazole*-2-*yl*)*phenyl*]–20-(4-bromophenyl)-porphyrinate was also obtained.** Eluent: 50:1 DCM/methanol mixture. Yield: 44 mg (80%), vinous-green crystalline powder. UV-visible: λ_{max}, nm (log ε): 427 (5.98); 553 (4.81); 597 (4.65) (dichloromethane). ^{1}H NMR δ, ppm: 7.36–7.42 m (6H); 7,65br.s (3H); 7,72br.s (3H); 7,88d (2H, 3 J = 8,2 Hz); 8,06d (2H); 8,36br.d (6H); 8,54br.d (6H); 8,93–9,01 m (8H) ($CDCl_3$).

MALDI-TOF MS: *m/z* calculated: $C_{65}H_{36}BrN_7O_3Zn$: 1105.14; determined experimentally: 1105,05 $[M]+$.

2.2.5. Synthesis of 5,10,15,20-tetraphenylporphin (III)

Porphyrin **(III)** was synthesized according to the procedure described in [10]. ^{1}H NMR δ, ppm: 8,90 s (8H, β-H); 8,24–8,29 m (8H, 2,6-H-pH); 7,76–7,84 m (12H, 3,4,5-H-pH); −2,72bs (2H, NH) ($CDCl_3$). UV-visible: λ_{max}, nm (lgε): 647(3.82), 590(3.86), 550(4.03), 515(4.27), 418(5.67) ($CHCl_3$).

MALDI-TOF MS: *m/z* calculated: C44H30N4, 614.4011; determined experimentally: 614.6065 $[M]+$.

The additional data are presented in Figs. 1S-6S in Supplementary material. additional material is presented in Figs. 1-6

дополнительный материал представлен на рисунках 1–6. dopoleitelny material represented drawings 1–6

дополеительный материал представлен рисунками 1–6

Не удалось загрузить все результаты.

Повторить

Повторная попытка…

Повторная попытка…

The quantum-chemical calculations for these compounds were performed using the Gaussian 9 software package [24]. The 3–21 G basis set was used to describe the electron-wave functions of atoms was borrowed from the EMSL library [25,26]. The calculations for these compounds were made by the DFT method using the B3LYP hybrid functional. Initially, during the porphyrin macrocycle construction, the angles and bonds of the averaged structure of porphyrins were used. A nitrogen atom with a lone electron pair was installed in such a way that the lone electron pair would be directed towards the coordination center. Joint structures have been fully optimized with no symmetry constraints. After the optimization of the geometric parameters, the wave function stability was tested.

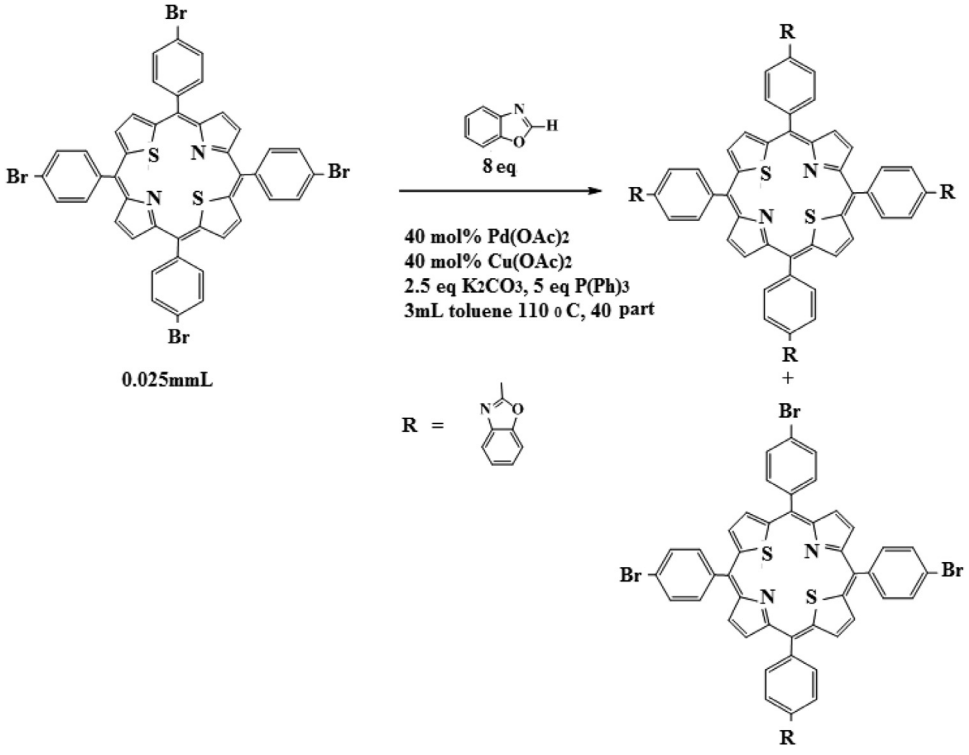

Scheme 3. The third stage.

3. Results and discussion

An important part of the synthesis procedure of heterosubstituted porphyrins is preparation of initial semi-products. The procedure of 5,10,15,20-tetrakis[4′-(*benzoxazole*-2-*yl*)*phenyl*]−21,23-dithiaporphyrin synthesis included three main stages. At first, the reaction of thiophen with *n*-butyllithium produced an organolithium compound that later interacted with a 4-bromobenzaldehyde solution in tetrahydrofuran (THF) and formed 2,5-bis(4′bromophenylhydroxymethyl)thiophen with a 75% yield (scheme 1).

An analysis of the literature data [27,28] shows that the synthesis duration and the yield of heterosubstituted porphyrins to a large extent depend on the medium of the condensation reaction. For example, Ullman and Manassen [27] demonstrated that substitution of benzene containing 2% chloroacetic acid for toluene reduced the reaction duration by a third and increased the product yield from 6 to 10%. The use of *p*-xylene with trifluoroacetic acid (TFA) additions as the solvent made it possible to significantly shorten the synthesis procedure (scheme 2) required to prepare 5,10,15,20-tetrakis[4′-*bromophenyl*]−21,23-dithiaporphyrin with a 12% yield.

Further modification of 5,10,15,20-tetrakis[4′-*bromophenyl*]−21,23-dithiaporphyrin employed metal complex catalysis reactions, namely C–H-functionalization of the hetarylating macrocycle. Benzoxazole with an "acidic" C–H bond served as such hetarylating agent.

The reaction was carried out with a $Pd(OAc)_2/Cu(OAc)_2$ catalytic system (40/40 mol%) in the presence of 2.5 eq. triphenylphosphine as the ligand and 5 eq. K_2CO_3 in boiling toluene and lasted for 40 h.

In contrast to a similar tetraphenylporphyrin (TPP) reaction with the main heteroarylation product being trihetaryl-substituted TPP with a small amount of 5,10,15,20-tetrakis[4′-(*benzoxazole*-2-*yl*)*phenyl*]porphyrin [13], in this case, the yield of the product – 5,10,15,20-tetrakis[4′-*benzoxazole*-2-*yl*)*phenyl*]−21,23-dithiaporphyrin – reached 46%. Another product, which was extracted by monohetarylation, retained three bromine atoms, and its yield was 10% (scheme 3).

The calculations of the geometric parameters for these compounds were carried out by the DFT method using the B3LYP hybrid functional (Table 1). The calculation results showed that the substitution of the sulfur atoms for nitrogen atoms in the macrocycle reaction center increased the lengths of the bonds between the corresponding carbon and the heteroatom. This is the reason for the radial deformation of tetrapyrrole macrocycle (**I**). The introduction of peripheral substituents into compounds (**I**) and (**II**) caused out-of-plane distortions of the macrocycles (Fig. 1), in the form of a ruffled macrocycle conformation. Ruffled conformations are characterized by in-plane rotation of the pyrrole rings and significant out-of-plane displacements of the *meso*–carbon atoms. It is known that the noted structural changes also indirectly affect the electronic structure of the macrocycle, decreasing its aromaticity and increasing the electron density at the atoms of the porphyrin coordination center.

It is known that porphyrins (H_2P) and their heterosubstituted analogues can be protonated in organic solvents in the presence of acids at the transannular nitrogen atoms [29,30].

The basic properties of heterosubstituted perchloric acid ligand (**I**) in comparison with classical porphyrin analogue (**II**) and unsubstituted TPP (**III**) were studied by the spectrophotometric titration method in an acetonitrile – perchloric acid system at $T = 298$ K.

To a first approximation (with no solvent involved and without stabilization of the resulting particles by counterions), the acid-base interaction processes of porphyrins and related macrohetero-

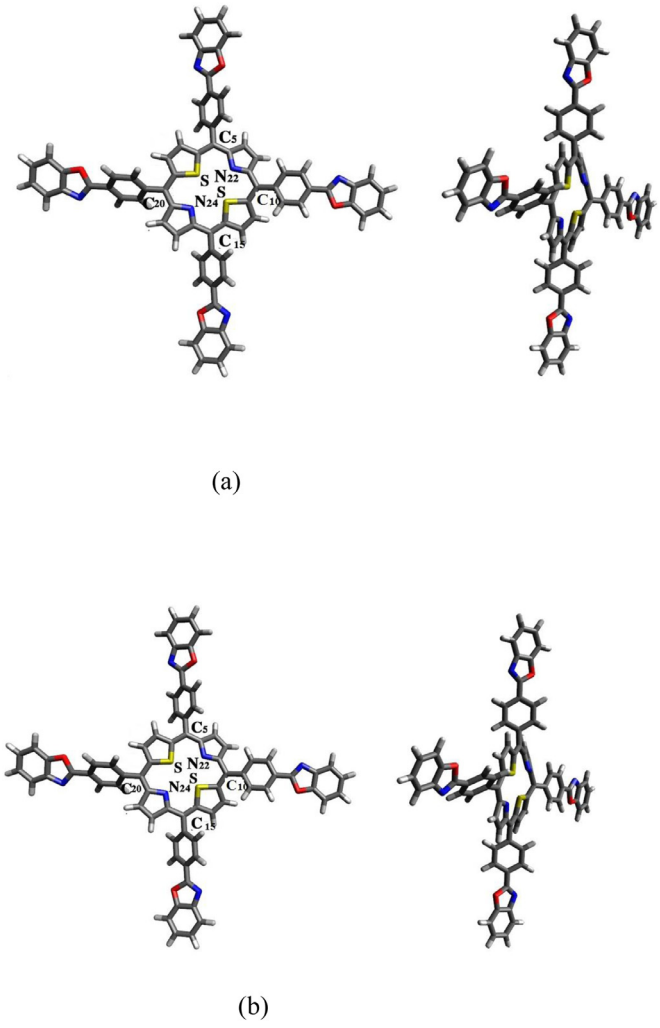

Fig. 1. Optimized structures of (a) (**I**), (b) (**II**), obtained by DFT calculations at the B3LYP/3–21 G level of theory.

Table 1
Geometric parameters of compounds (**I**) and (**II**).

Compound (**I**) bond length Å		Compounds (**II**)	
$C_3 - C_2$	1.423	$C_3 - C_2$	1.392
$C_2 - C_1$	1.387	$C_2 - C_1$	1.387
$C_3 - C_4$	1.390	$C_3 - C_4$	1.388
$C_4 - C_1$	2.533	$C_4 - C_1$	2.263
$C_4 - S$	1.729	$C_3 - N_{21}$	1.384
$C_1 - S$	1.727	$C_1 - N_{21}$	1.384
$C_{18} - C_{19}$	1.447	$N_{21} - H$	1.012
$C_{18} - C_{17}$	1.334	$C_{18} - C_{19}$	1.465
$C_{17} - C_{16}$	1.473	$C_{18} - C_{17}$	1.329
$C_{19} - C_{16}$	2.165	$C_{17} - C_{16}$	1.487
$C_{19} - N_{24}$	1.374	$C_{19} - C_{16}$	2.161
$C_{16} - N_{24}$	1.300	$C_{19} - N_{24}$	1.391
$S - N_{24}$	3.056	$C_{16} - N_{24}$‘	1.304
$N_{24} - N_{22}$	4.520	$N_{24} - N_{22}$	4.199
Angles, degrees			
$C_{20} - C_1 - S - C_4$	171.9	$C_{20} - C_1 - N_{21} - H$	8.0
$C_{20} - C_{19} - N_{24} - C_{16}$	176.1	$H - N_{21} - C_1 - C_2$	−178.3
$C_2 - C_1 - C_{20} - C_{19}$	−174.3	$H - N_{21} - C_4 - C_5$	−1.9
$C_1 - S - C_4 - C_5$	−172.8	$H - N_{21} - C_4 - C_3$	179.4
$C_4 - S - C_1$	94.3	$C_4 - N_{21} - C_1$	109.7
$C_1 - C_{20} - C_{19}$	121.7	$C_1 - C_{20} - C_{19}$	125.5
$C_{19} - N_{24} - C_{16}$	108.1	$C_{19} - N_{24} - C_{16}$	106.6

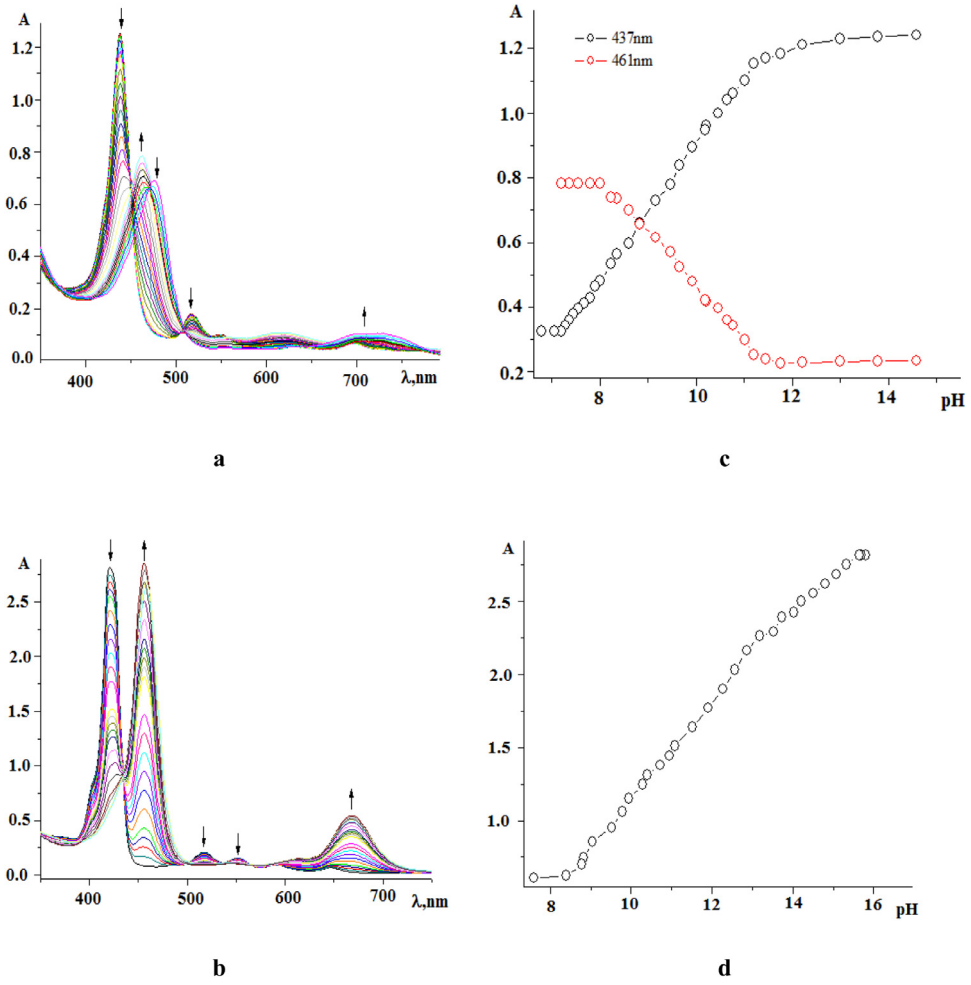

Fig. 2. Changes in the UV-visible spectra in the acetonitrile – perchloric acid system in the process of titration with perchloric acid in acetonitrile at 298 K of: a) compound (**I**) (C_{porph} = 6.30•10⁻6 mol/L), b) compound (**II**) (C_{porph} = 3.07•10⁻5 mol/L) in the acetonitrile – perchloric acid system; c) respective titration curves of compound (**I**) with the analytical wavelengths of 437 and 461 nm; d) respective titration curve of compound (**II**) with the analytical wavelength of 421 nm.

cycles in acidic media can be described by Eqs. (1-2) [31]:

$$H_4P^{2+} \underset{\rightleftarrows}{K_{b1}} H_3P^+ + H^+ \quad (1)$$

$$H_3P^+ \underset{\rightleftarrows}{K_{b2}} H_2P + H^+ \quad (2)$$

where H_2P, H_3P^+, and H_4P^{2+} are the molecular, mono- and doubly-protonated ligand forms (the notation for classical porphyrins (**II**) and (**III**), for compound (**I**) was used: S_2P, HS_2P^+, and $H_2S_2P^{2+}$, respectively).

The spectrophotometric studies of compounds (**I**) and (**II**) in the acetonitrile – perchloric acid system showed that as the perchloric acid concentration increased, two families of spectral curves were formed in the electronic absorption spectra, each with its own set of isobestic points. These experimental data confirm that there were two stages in the protonation process. The changes in the UV-visible spectra during the titration and the titration curves are shown in Fig. 2. By distinguishing the two families of isobestic points on the UV-visible spectra, we were able to determine the concentration intervals of existence (of protonated forms (**I**) and (**II**)) and spectral characteristics of the intermediate mono-protonated form for HS_2P^+ (Fig. 3). The parameters of the UV-visible spectra of the molecular and resulting protonated forms are given in Table 2.

The total values of the basic ionization constants of protonated forms (**I**) in comparison with their classical analogue – H_2TPP – in the acetonitrile – perchloric acid system at 298K were determined by Eq. (3); their values are given in Table 2.

$$pK_b = -\lg K_b = pH - -\lg Ind \quad (3)$$

Here, K_b is the basicity constant at the first and second steps, *Ind* is the indicator ratio for compound (**I**) at the first $[S_2P]/[HS_2P^+]$ and second $[HS_2P^+]/[H_2S_2P^{2+}]$ protonation steps, respectively, for compound (**II**) – $[H_2PP]/[H_3PP^+]$ $[H_3PP^+]/[H_4PP^{2+}]$ – the pH values were calculated by the method described in [23] by formula (4):

$$pH = -2.48 - 2.65 \lg C_{HC104} \quad (4)$$

The error in the calculation of the constants during the experiment did not exceed 3–5%.

Taking into account the processes of basic dissociation of protonated forms (1–2), and material-balance Eq. (5), as well as the proportionality of the optical density of the dissolved substance to its concentration, according to the Lambert–Bouguer–Beer law, we determined the distribution of the concentrations of the molecular and protonated forms of the studied compound in titration processes (6–9) (Fig. 2 for compound (**I**)).

$$C^0 = C_{S_2P} + C_{HS_2P^+} + C_{H_2S_2P^{2+}} = 100\% \quad (5)$$

$$At = \frac{A_{S_2P} \cdot K_{b1} \cdot K_{b2} + A_{HS_2P^+} \cdot 10^{-pH} \cdot K_{b1} + 10^{(-pH)2} \cdot A_{H_2S_2P^{2+}}}{K_{b1} \cdot K_{b2} + 10^{-pH} \cdot k_{b2} + 10^{(-pH)^2}} \quad (6)$$

Table 2
Indicators of base ionization constants and spectral characteristics of molecular and protonated forms of porphyrins (**I**) – (**III**) in the acetonitrile – perchloric acid system at $T = 298$ K.

Porphyrin	λ(lgε*)					pK_1	pK_2	ΣpK
H_2TPP	413(5.02)	512(3.56)	546(3.12)	589(2.92)	646(2.96)	–	–	19.80[26]
H_4TPP^{2+}	441(5.04)	–	–	–	661(4.17)			
S_2TPP	437(5.3)	518(4.46)	549sh(4.20)	635(3.99)	698(4.05)	9.88	9.85	19.73
HS_2TPP^{+}	463(5.1)	–	616(4.25)	707(4.17)				
$H_2S_2TPP^{2+}$	475(5.04)	704(4.23)	–	733sh(4.23)				
H_2PP	421(4.96)	516(3.84)	553(3.70)	591(3.51)	647(3.37)	12.30	10.01	22.31
H_4PP^{2+}	456(4.97)	–	–	614sh(3.70)	667(4.25)			

* ε ((mol/L)$^{-1}$.cm^{-1}) is the molar absorption coefficient (molar extinction coefficient); the error in three parallel series of experiments was 1–3%.

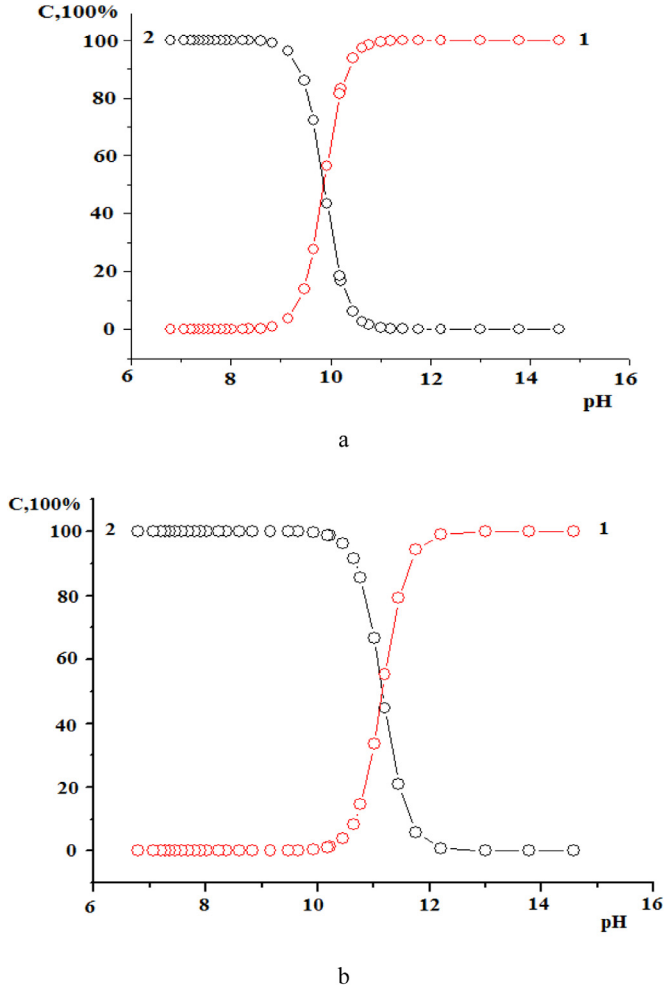

Fig. 3. Distribution of concentrations and spectra of the molecular (1) and doubly protonated (2) forms during the titration of compound (**I**) (a) and compound (**II**) (b).

$$C_{S_2P} = \frac{k_{b1} \cdot k_{b2}}{k_{b1} \cdot k_{b2} + 10^{-pH} \cdot k_{b2} + 10^{(-pH)^2}} \cdot 100\% \quad (7)$$

$$C_{HS_2P^+} = \frac{10^{-pH} \cdot k_{b2}}{k_{b1} \cdot k_{b2} + 10^{-pH} \cdot k_{b2} + 10^{(-pH)^2}} \cdot 100\% \quad (8)$$

$$C_{H_2S_2P^{2+}} = \frac{10^{(-pH)^2} \cdot k_{b2}}{k_{b1} \cdot k_{b2} + 10^{-pH} \cdot k_{b2} + 10^{(-pH)^2}} \cdot 100\% \quad (9)$$

Here: C_{S2P}, $C_{HS2P}{}^{+}$, $C_{H2S2P}{}^{2+}$ are the concentrations of the neutral and ionized forms of porphyrin (**I**) or C_{H2P}, $C_{H3P}{}^{+}$, $C_{H4P}{}^{2+}$ for porphyrin (**II**)); K_{b1} and K_{b2} are the basicity constants of processes (1) and (2); A_t, A_{S2P}, $A_{HS2P}{}^{+}$, $A_{H2S2P}{}^{2+}$ are the optical densities of the solutions corresponding to the neutral and ionized forms of porphyrin (**I**) or A_{H2P}, $A_{H3P}{}^{+}$, $A_{H4P}{}^{2+}$ for porphyrin (**II**)).

The introduction of bulky substituents into the *para*- positions of the four phenyl fragments of compound (**II**) increases the basic properties of the ligand in comparison with H_2TPP due to additional deformation of the macrocycle.

Further modification of compound (**II**), namely the replacement of two pyrrole nitrogen atoms of the reaction center with more electropositive sulfur atoms, as could be expected, reduces the basic properties of compound (**I**) by ~ 2.5 orders of magnitude in comparison with (**II**). However, it should be said that in comparison with H_2TPP, the basicity of (**I**) becomes only slightly lower (the changes are within the experimental error). This fact is evidently associated with the mutually opposing action of several factors: the electron effect of the benzoxazole substituent and increase in the macrocycle deformation because of the bigger diameter of the transannular sulfur atoms in comparison with nitrogen [32,33]. Both factors make the compound basic properties stronger (**I**). Lower basicity, *i.e.* partial negative charges on the central nitrogen atoms, causes redistribution of the electron density due to the introduction of less electronegative sulfur atoms.

4. Conclusion

In summary, the present study provides an insight into the design of the classical and heterosubstituted ligand of porphyrin-inspired macrocycles. The reaction of metal complex catalysis was used to synthesize 5,10,15,20-tetrakis[4′-(*benzoxazole*-2-*yl*)*phenyl*]–21,23-dithia (**I**) and 5,10,15,20-tetrakis[4′-(*benzoxazole*-2-*yl*)*phenyl*]porphyrin (**II**). The geometric parameters for these compounds were calculated by UV-visible spectroscopy. The UV-visible spectra show that there is distinct stepwise protonation in both porphyrins. The molecular and resulting protonated forms were characterized by absorption spectra.

Declaration of Competing Interest

The authors declare that they have no known competing financial interests or personal relationships that could have appeared to influence the work reported in this paper.

CRediT authorship contribution statement

S.G. Pukhovskaya: Conceptualization, Methodology, Software, Data curtion. **Y.B. Ivanova:** Visualization, Investigation, Writing – original draft. **A.N. Kiselev:** Writing – review & editing. **N.A. Fomina:** Software, Validation. **S.A. Syrbu:** Supervision.

Acknowledgements

The work was financially supported by the Russian Foundation for Basic Research, grant No. 19–03–00214 A, and was carried out on the equipment of the Upper Volga Region Center of Physico-Chemical Research.

Supplementary materials

Supplementary material associated with this article can be found, in the online version, at doi:10.1016/j.molstruc.2021.130406.

References

[1] B.D. Berezin, Coordination Compounds of Porphyrins and Phthalocyanines, Wiley, New York, 1981.
[2] G.P. Gurinovich, K.N. Sevchenko, Spectroscopy of Chorophyll and Related Compounds, Minsk, 1968 in Russ..
[3] M.R. Tarasevich, M.R. Radyushkina, Catalysis and Electrocatalysis By Metalloporphyrins, Moscow, Mir, 1982. (in Russ.).
[4] Dao Tkhe Nam, Yu.B. Ivanova, S.G. Puhovskaya, M.M. Kruk, Acid–base equilibria and coordination chemistry of the 5,10,15,20-tetraalkyl-porphyrins: implications for metalloporphyrin synthesis, RSC Adv 5 (2015) 26125–26131, doi:10.1039/C5RA01323B.
[5] Yu.B. Ivanova, S.G. Pukhovskaya, N.Zh. Mamardashvili, O.I. Koifman, M.M. Kruk, Rate-acidity hysteresis and enthalpy-entropy compensation upon metalloporphyrin formation: implication for the metal ion coordination mechanism, J. Molec. Liquids. 275 (2019) 491–498, doi:10.1016/j.molliq.2018.11.107.
[6] O.I. Koifman, Functional Materials On the Basis of Tetrapyrrolic Macroheterocycles, LENAND, Moscow, 2019 in Russ..
[7] Maria da, G.H. Vicente, Kevin M. Smith, Syntheses and Functionalizations of Porphyrin Macrocycles, Curr Org Synth 11 (2014) 3–28, doi:10.2174/15701794113106660083.
[8] S.A. Syrbu, T.A. Ageeva, E.A. Kolodina, A.S. Semeykin, O.I. Koifman, Strategies for the synthesis of porphyrin monomers, J. Porphyrins Phthalocyanines. 10 (2006) 885 http://dx.doi.org/10.1142/S1088424606000235.
[9] R. Takahashi, Y. Kobuke, Hexameric macroring of gable-porphyrins as a light-harvesting antenna mimic, J. Am. Chem. Soc. (125) (2003) 2372–2373, doi:10.1021/ja028325y.
[10] J.S. Lindsey, Synthesis of meso-Substituted Porphyrins, in: K.M. Kadish, K.M. Smith, R. Guilard (Eds.), The Porphyrin Handbook, Academic Press, San Diego, 2000, pp. 45–118.
[11] L. Latos-Gra˙zyński, Core-Modified Heteroanalogues of Porphyrins and Metalloporphyrins, in: K.M. Kadish, K.M. Smith, R. Guilard (Eds.), The Porphyrin Handbook, Academic Press, New York, 2000, pp. 361–417.
[12] I.P. Beletskaya, V.S. Turin, A. Uglov, C. Stern, R. Guilard, Survey of Synthethic Routes for Synthesis and Substitution in Porphyrins, in: K.M. Kadish, K.M. Smith, R. Guilard (Eds.), The Handbook of Porphyrin Science, World Scientific Publishing, Singapore, 2012, pp. 5–258.
[13] A.N. Kiselev, O.K. Grigorova, A.D. Averin, S.A. Syrbu, O.I. Koifman, I.P. Beletskaya, Direct catalytic arylation of heteroarenes with *meso*-bromophenylsubstituted porphyrins, Beilstein J. Org. Chem 13 (2017) 1524–1532, doi:10.3762/bjoc.13.152.
[14] V. Faraon, R.M. Ion, Ship-in-bottle porphyrin – zeolite nanomaterials, Optoelectron. Adv. Mat. 4 (2010) 1135–1140 https://oam-rc.inoe.ro/articles/ship-in-bottle-porphyrin-zeolite-nanomaterials/fulltext.
[15] C. Farren, S. FitzGerald, M.R. Bryce, A. Beeby, A. Batsanov, Synthesis, structure and optical characterisation of silicon phthalocyanine bis-esters, J. Chem. Soc., Perkin Trans. 2 (2002) 59–65, doi:10.1039/B108778A.
[16] M. Ethirajan, Y. Chen, P. Joshi, R.K. Pandey, The role of porphyrin chemistry in tumor imaging and photodynamic therapy, Chem. Soc. Rev. 40 (2011) 340–362, doi:10.1039/B915149B.
[17] A. Gyulkhandanyan, L. Gyulkhandanyan, R. Ghazaryan, F. Fleury, M. Angelini, G. Gyulkhandanyan, V. Sakanyan, Assessment of new cationic porphyrin binding to plasma proteins by planar microarray and spectroscopic methods, J. Biomol. Struct. Dyn. 3 (2013) 363–375, doi:10.1080/07391102.2012.703063.
[18] H. Horiuchi, M. Hosaka, H. Mashio, M. Terata, S. Ishida, S. Kyushin, T. Okutsu, T. Takeuchi, H. Hiratsuka, Silylation improves the photodynamic activity of tetraphenylporphyrin derivatives *in vitro* and *in vivo*, Chem. Eur. J. 20 (2014) 6054–6060, doi:10.1002/chem.201303120.
[19] David G. Hilmey, Masako Abe, Marina I. Nelen, Water-Soluble, Core-Modified Porphyrins as Novel, Longer-Wavelength-Absorbing Sensitizers for Photodynamic Therapy. II Effects of Core Heteroatoms and *Meso*-Substituents on Biological Activity, J. Med. Chem. 45 (2002) 449–461, doi:10.1021/jm0103662.
[20] S.M. Rida, F.A. Ashour, S.A. El-Hawash, M.M. ElSemary, M.H. Badr, M.A. Shalaby, Synthesis of some novel benzoxazole derivatives as anticancer, antiHIV-1 and antimicrobial agents, Eur. J. Med. Chem. 40 (2005) 949–959, doi:10.1016/j.ejmech.2005.03.023.
[21] L. Wang, P. Zhang, X. Zhang, Y. Zhang, Y. Li, Y. Wang, Synthesis and biological evaluation of a novel series of 1,5-benzothiazepine derivatives as potential antimicrobial agents, Eur. J. Med. Chem. 44 (2009) 2815–2821, doi:10.1016/j.ejmech.2008.12.021.
[22] A. Weissberger, E. Proskauer, J. Riddick, Organic solvents: Physical Properties and Methods of Purification, Wiley, New York, 1955.
[23] S.G. Pukhovskaya, Yu.B. Ivanova, Dao The Nam, A.S. Vashurin, Dependence of the basic properties of *meso*-nitro-substituted derivatives of β-octaethylporphyrin on the nature of substituents, Russ. J. of Phys. Chem. 88 (2014) 1670–1676, doi:10.1134/S0036024414100288.
[24] M.J. Frisch, G.W. Trucks, H.B. Schlegel, G.E. Scuseria, M.A. Robb, J.R. Cheeseman, G. Scalmani, V. Barone, B. Mennucci, G.A. Petersson, H. Nakatsuji, M. Caricato, X. Li, H.P. Hratchian, A.F. Izmaylov, J. Bloino, G. Zheng, J.L. Sonnenberg, M. Hada, M. Ehara, K. Toyota, R. Fukuda, J. Hasegawa, M. Ishida, T. Nakajima, Y. Honda, O. Kitao, H. Nakai, T. Vreven, J.A. Montgomery, J.E. Peralta, F. Ogliaro, M. Bearpark, J.J. Heyd, E. Brothers, K.N. Kudin, V.N. Staroverov, R. Kobayashi, J. Normand, K. Raghavachari, A. Rendell, J.C. Burant, S.S. Iyengar, J. Tomasi, M. Cossi, N. Rega, J.M. Millam, M. Klene, J.E. Knox, J.B. Cross, V. Bakken, C. Adamo, J. Jaramillo, R. Gomperts, R.E. Stratmann, O. Yazyev, A.J. Austin, R. Cammi, C. Pomelli, J.W. Ochterski, R.L. Martin, K. Morokuma, V.G. Zakrzewski, G.A. Voth, P. Salvador, J.J. Dannenberg, S. Dapprich, A.D. Daniels, Ö. Farkas, J.B. Foresman, J.V. Ortiz, J. Cioslowski, D.J. Fox, Gaussian 09, Revision D.01, Gaussian Inc. Wallingford CT, 2009.
[25] D. Feller, The role of databases in support of computational chemistry calculations, J. Comp. Chem. 17 (1996) 1571–1586 10.1002/(SICI)1096-987X(199610)17:13≤1571::AID-JCC9≥3.0.CO;2.
[26] K.L. Schuchardt, B.T. Didier, T. Elsethagen, L. Sun, V. Gurumoorthi, J. Chase, J. Li, T.L. Windus, Basis set exchange: a community database for computational sciences, J. Chem. Inf. Model. 47 (2007) 1045–1052, doi:10.1021/ci600510j.
[27] A. Ulman, J. Manassen, Synthesis of new tetraphenylporhyrin molecules containing heteroatoms other than nitrogen, J. Amer. Chem. Soc. 97 (1975) 6540–6544, doi:10.1021/ja00855a042.
[28] Iti Gupta, M. Ravikanth, Recent developments in heteroporphyrins and their analogues, Coord. Chem. Rev. 250 (2006) 468–518, doi:10.1016/j.ccr.2005.10.010.
[29] S.A. Syrbu, Y.B. Ivanova, S.G. Pukhovskaya, A.S. Vashurin, Spectrophotometric Study of Acid-Base Properties of Sulfonated Derivatives of 5,10,15,20-Tetraphenyl-21-thiaand 5,10,15,20-Tetraphenyl-21-oxoporphyrins in the Ethanol–Sulfuric Acid System, Russ. J. Gen. Chem. 89 (2019) 255–260, doi:10.1134/S1070363219020142.
[30] S.G. Pukhovskaya, Yu.B. Ivanova, M.I. Razumov, A.O. Plotnikova, D.A. Shelekhova, A.S. Vashurin, S.A. Syrbu, J. Incl. Phenom. Macrocycl. Chem. (2020), doi:10.1007/s10847-020-00981-4.
[31] V.G. Andrianov, O.V. Malkova, Acid-base properties of porphyrins in non-aqueous solutions, Macroheterocycles 2 (2009) 130–138, doi:10.6060/mhc2009.2.130.
[32] O.A. Golubchikov, S.G. Pukhovskaya, E.M. Kuvshinova, Structures and properties of spatially distorted porphyrins, Russ. Chem. Rev. 74 (2005) 249–264, doi:10.1070/RC2005v074n03ABEH000925.
[33] Yu.B. Dao Tkhe Nam, S.G. Ivanova, M.M. Puhovskaya, S.A. Kruk, Syrbu, Acid-base Equilibria and coordination Chemistry of the 5,10,15,20-tetraalkylporphyrins: implications for Metalloporphyrin Synthesis and sensor design, RSC Adv 33 (2015) 26125–26131, doi:10.1070/RC2005v074n03ABEH000925.